Eur Radiol (2011) 21:2255–2260
DOI 10.1007/s00330-011-2180-9

CHEST

Malignant versus benign mediastinal lesions: quantitative assessment with diffusion weighted MR imaging

Sevtap Gümüştaş · Nagihan İnan · Hasan Tahsin Sarisoy · Yonca Anik · Arzu Arslan · Ercüment Çiftçi · Gür Akansel · Ali Demirci

Received: 19 November 2010 / Revised: 3 May 2011 / Accepted: 6 May 2011 / Published online: 23 June 2011

Abstract
Objectives We aimed to evaluate the performance of diffusion-weighted magnetic resonance imaging in differentiating malignant from benign mediastinal lesions.
Methods Fifty-three mediastinal lesions were examined with T1- and T2-weighted (W) conventional images. Then, two diffusion-weighted images were obtained with $b=0$ and 1000 s/mm² values and apparent diffusion coefficients (ADC) were calculated. The statistical significance of differences between measurements was tested using the Student-*t* test.
Results The mean ADC of malignant lesions was significantly lower than that of the benign masses ($p<0.001$). The cut-off value of $\leq 1.39\times10^{-3}$ mm²/s indicated a malignant lesion with a sensitivity of 95% and specificity of 87%.
Conclusion Diffusion-weighted imaging may be helpful in differentiating benign from malignant mediastinal masses.

Keywords Diffusion-weighted MR imaging · Mediastinal lesions · Differentiation · Apparent diffusion coefficients (ADC) · Magnetic resonance imaging

Introduction

Mediastinal masses span a wide histopathological and radiological spectrum. While relatively specific imaging clues exist for certain lesions such as thyroid masses and cysts, many solid malignant and benign lesions appear remarkably similar on computed tomography (CT) and magnetic resonance imaging (MRI) [1–4]. Correct identification of these masses is essential in order to administer appropriate treatment. Despite being the most common modality for imaging the mediastinum, CT cannot be used to reliably differentiate benign from malignant lesions of this anatomical region [5–7]. MRI, on the other hand, presents valuable diagnostic information in assessing the mediastinum owing to its ability to provide excellent soft tissue detail. In addition, special applications have been developed over recent years that unveil minute metabolic and biophysical differences between tissues [8, 9]. Diffusion-weighted magnetic resonance imaging (DWI) is one such technique, which explores the translational mobility of water molecules, thereby shedding light on the microstructural features of the tissue of interest, whether they facilitate, or restrict such freedom of proton mobility. DWI has been primarily used in neuroradiology, but applications in other body areas have also been increasing. Fast imaging techniques such as echo-planar imaging (EPI) facilitate the use of DWI in thoracic imaging by decreasing the deleterious effects of motion [10, 11]. Nevertheless, the number of studies using DWI in mediastinal pathology is somewhat limited [12]. The purpose of this study was to investigate the differentiation of malignant from benign mediastinal lesions on DWI.

Materials and methods

Patients

The study was approved by our institutional review board and protocol review committee. Because the tests used were

S. Gümüştaş (✉) · N. İnan · H. T. Sarisoy · Y. Anik · A. Arslan · E. Çiftçi · G. Akansel · A. Demirci
Department of Radiology, School of Medicine,
University of Kocaeli,
Kocaeli Uni. Tip Fak Radyoloji AD,
41380 Umuttepe Kocaeli, Turkey
e-mail: svtgumustas@hotmail.com

part of the routine clinical workup of these patients, informed consent was not required by the review board. We obtained blanket consent from all patients for the use of their findings for research and educational purposes, with patient privacy secured.

From May 2008 to June 2010, 44 consecutive patients (25 males, 19 females) with 53 mediastinal lesions detected on chest CT were referred for MRI in our hospital and included in this prospective study according to our entry criteria.

Our entry criteria were as follows; (a) a solid mediastinal nodule or mass. Typical thyroidal masses and vascular lesions were excluded. Lesions containing large amounts of necrosis or calcification were also excluded; (b) lesions size >15 mm in diameter in view of the limited planar resolution of DWI; (c) presence of a certain proven diagnosis based on histopathological, clinical or follow-up findings; (d) no chemotherapeutic or radiotherapeutic treatment currently being applied; and (e) no contra-indications for MRI were present and the patient was able to tolerate the examination.

Magnetic resonance imaging

All patients were examined using a 3 Tesla MR unit (Philips Achieva Intera Release, Eindhoven, The Netherlands), with a four-element phased-array body coil. All patients initially underwent a routine MRI session for the thorax that included: axial T1-weighted (W) breath-hold turbo field echo (TFE) with and without fat suppression (TR/TE/FA/NEX:10/2.3/15/1) and axial T2-W single-shot turbo spin echo (SS-TSE) (TR/TE/NEX/TSE factor: 1536/80/1/73). Fat suppression was performed by using spectral attenuated inversion recovery (SPAIR) imaging with inversion time of 180 ms. Subsequently, four series of axial single-shot spin-echo echo-planar (SS-SE-EPI) DWIs (echo-planar imaging factor, 57; TR/TE/NEX: 1720/68/2; we used sensitizing gradients in x, y, and z directions in order to obtain isotropic diffusion weighting) were acquired using the b values 0 and 1000 s/mm². Apparent diffusion coefficient (ADC) maps were reconstructed from the b 0 and b 1000 s/mm² images. MRI, including DWI, consisted of a multisection acquisition with a slice thickness of 6 mm, an intersection gap of 1 mm, and an acquisition matrix of 140×108. The field of view varied between 455 and 500 mm. All sequences were acquired using a partially paralel imaging acquisition and SENSE (sensitivity encoding) reconstruction with a reduction factor (R) of 2. Each one of the b values was obtained during a single breath-hold and the examination time was 26 s for each b value acquisition.

Quantitative analysis

Quantitative measurements were made using a dedicated workstation (Dell Workstation Precision 650, with the View Forum software platform provided by Philips Healthcare). All images were assessed by two radiologists (S.G., N.I.) who were blinded to the clinical history and results of the prior imaging studies. Each lesion was first evaluated on conventional images for location, size and the presence of cystic-necrotic parts. ADCs were then calculated from the ADC maps which were reconstructed from b 0 and b 1000 s/mm² values. For the evaluation of ADC, a region of interest (ROI) was placed on lesions centrally on the ADC maps. The size of the ROI was kept as large as possible, covering at least two- thirds of the lesion, yet avoiding interference from the surrounding lung tissue, major blood vessels and necrotic parts. This procedure was repeated three times for ADC calculation, and the average of the measurements was recorded as the final ADC.

Statistical analysis

The ADC values were compared between the groups. The Kolmogorov-Smirnov test showed that the data were normally distributed, so the differences in ADCs were analysed using the Student-t test. A p value of less than 0.05 was considered statistically significant. To evaluate the diagnostic performance of the mean ADC measurements in differentiating malignant from benign lesions and to describe the sensitivity and specificity, receiver operating characteristic (ROC) analysis was performed. An optimum cut-off point was hence determined as the value that best discriminates between the two groups in terms of maximum sensitivity and minimum

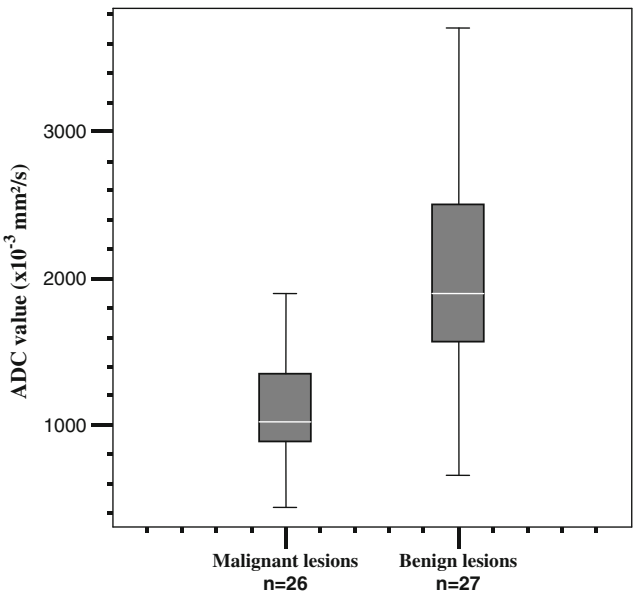

Fig. 1 Comparison of ADC values ($\times 10^{-3}$ mm²/s) from b1000 s/mm² in malignant and benign lesions. The mean ADC value of malignant lesions was significantly lower than those of benign lesions

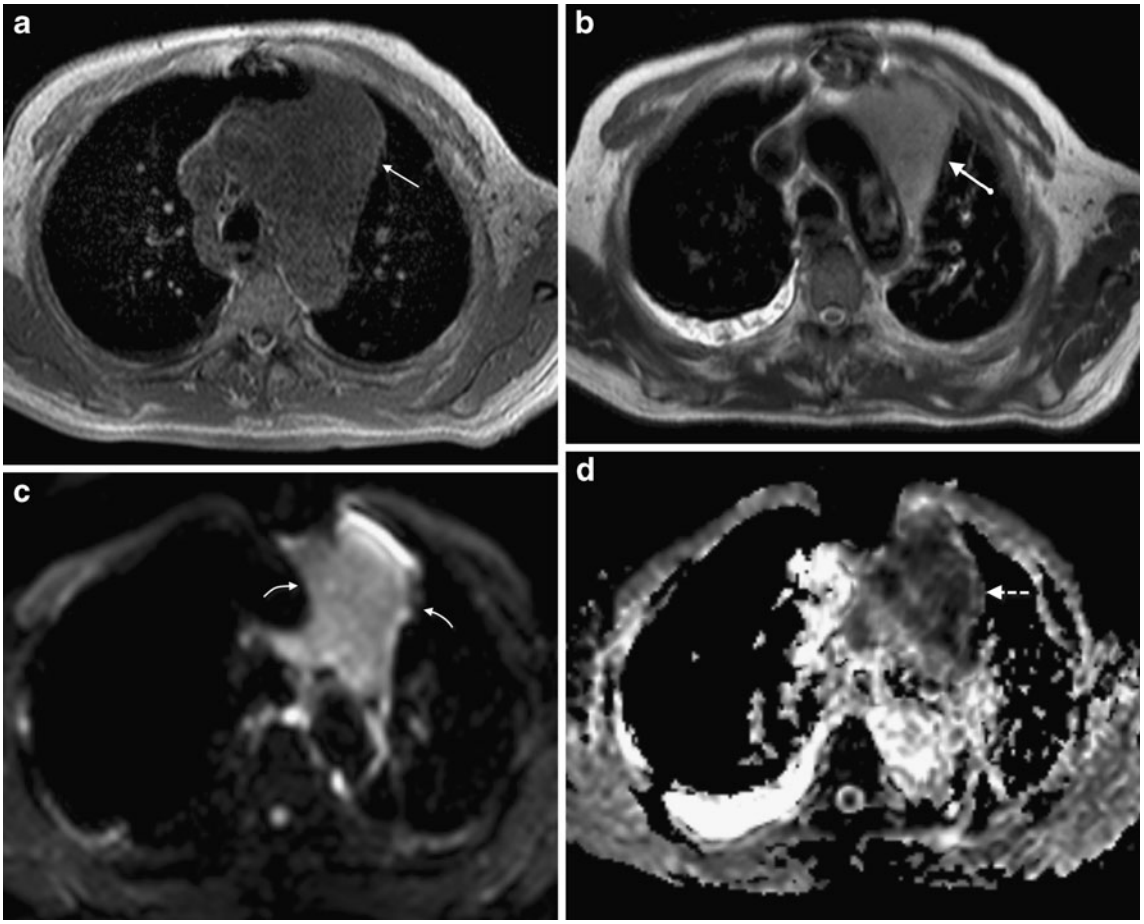

Fig. 2 Thymic non-Hodgkin lymphoma, a 71-year-old man with anterior mediastinal mass. **a** Transversal T1-W turbo field echo image shows the mass has hypointense signal and indistinguishable from vascular area (*arrow*) **b** The mass seems hyperintense on T2-W single shot turbo spin echo images (*thick arrow*) **c** Single-shot spin-echo echo-planar DW image with b 1000 s/mm² shows the mass has high signal intensity consistent with malignancy (*curved arrows*) **d** Notice the lesion shows significant low intensity on ADC map with low ADC value (0.43×10^{-3} mm²/s) (*dash arrow*)

number of false-positive results. All statistical analyses were performed using statistical software (SPSS version 15).

Results

Patients

The mean age of the entire group was 59±23 years (range: 2–88 years). The mean age of patients with benign masses was 40±20 years (range: 2–78 years) and of patients with malignant masses was 56±18 years (range: 13–88 years). The difference in age between groups was statistically significant (p=0.005).

The mean diameter of masses for the entire group was 32± 16 mm. The mean diameter of malignant lesions was 37± 18 mm (range: 17–80 mm) and of benign masses was 33± 25 mm (range: 15–120 mm). The difference in diameter between groups was not statistically significant (p=0.52).

Diagnosis

Two separate lesions were measured in 9 patients who had multiple lesions. Multiple lymph nodes were evaluated in 6 of these patients (2 patients with sarcoidosis, 1 with tuberculosis, 1 with psoriatic arthritis, 1 with Hodgkin lymphoma, 1 with leukaemia). In 2 patients with non-small cell lung cancer (NSCLCs) and 1 patient with esophageal cancer, the primary lesions and metastatic lymph nodes were measured separately. A single lesion was evaluated in the remainder of the patients.

Of 53 lesions, 26 were malignant and 27 were benign. The malignant lesions consisted of NSCLCs (n=11), lymphoma (n=9), leukemia (n=2), esophageal cancer (n=2), malignant neurogenic tumor (n=1), and metastatic lymphadenopathy from breast cancer (n=1). Lymphomas were Hodgkin lymphoma (n=6), and non- Hodgkin lymphoma (n=3). All cases with lung cancer presented with evident mediastinal components. The benign mediastinal masses consisted of

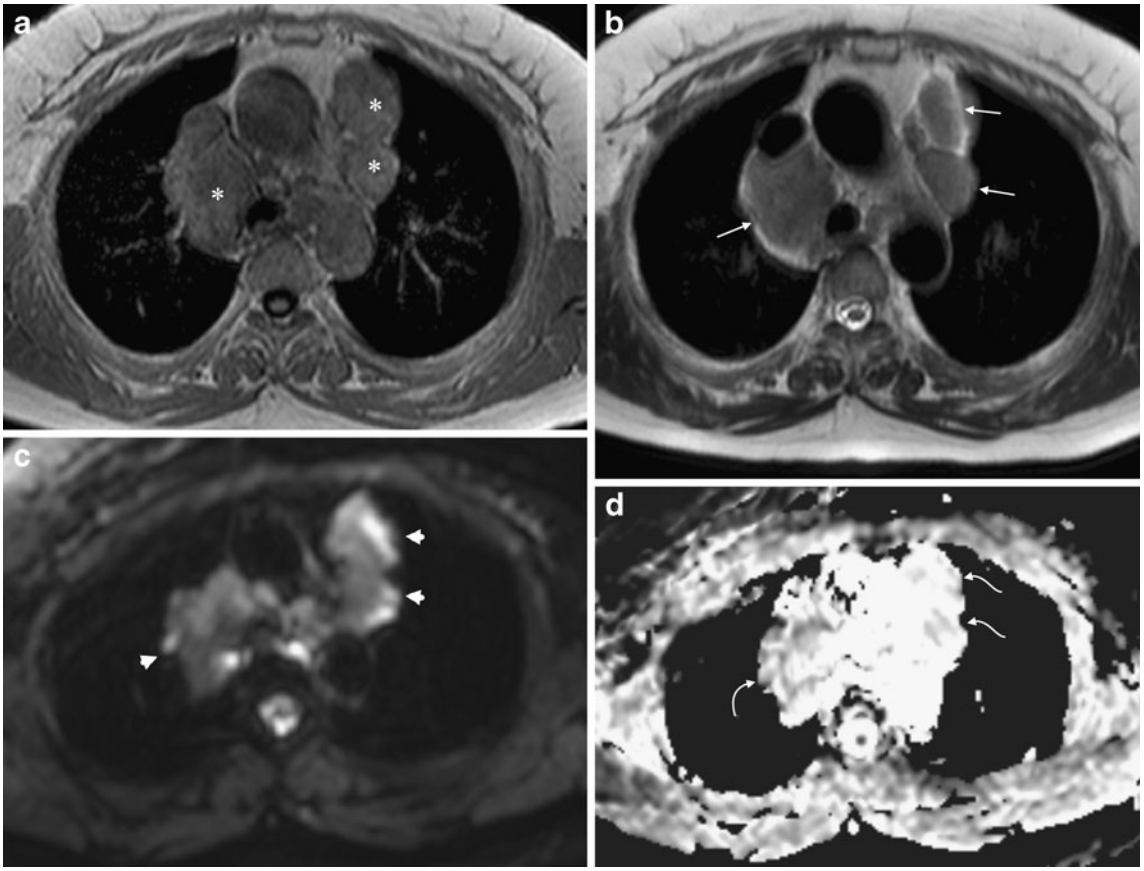

Fig. 3 Sarcoidosis, a 43-year-old woman with para aortic and right para tracheal lymphadenopathies. **a** Transversal T1-W turbo field echo image shows that signal intensities of lymphadenopathies are nearly isointense with the muscles (*asterixes*) **b** Transversal T2-W single shot turbo spin echo shows moderate signal intensity of lymphadenopathies (*arrows*) **c** Single-shot spin-echo echo-planar DW image with b 1000 s/mm² shows low-medium intensity of lesions (*arrow heads*) **d** ADC map from the b1000 s/mm², notice the lesions show significant high intensity of the masses (1.8×10^{-3} mm²/s) (*curved arrows*)

lymphadenopathies; caused by sarcoidosis (n=11), tuberculosis (n=3), psoriatic (n=2) and rheumatoid (n=1) arthritis, thymic hyperplasia (n=5), noninvasive thymoma (n=2), schwannoma (n=1), lipoma (n=1) and Riedel's thyroiditis (n=1).

Pathologic proof was available in 34 patients, through percutaneous biopsy in 18 and open surgery in 16. In all cases, MRI was performed prior to these procedures. The diagnosis was confirmed with radiological and clinical parameters in 10 patients. One lipoma was diagnosed on CT images and remained unchanged on radiological follow up. The clinical diagnoses in 4 cases with thymic hyperplasia were established by comparison to prior studies. In order to consider a lesion stable on follow-up, it was required to have remained unchanged for a minimum of 12 months. In 5 cases with sarcoidosis, the lesions showed significant regression after initiation of specific therapy.

Quantitative results

An ADC value could be measured for all lesions. The mean ADCs of malignant and benign lesions were $1.21\pm0.63\times10^{-3}$ mm²/s and $2.04\pm0.67\times10^{-3}$ mm²/s, respectively (Fig. 1). The mean ADC for the malignant group was significantly lower than that for the benign group (p<0.001).

The lowest ADC in the malignant group was detected in a patient with thymic large cell lymphoma ($0.4\pm0.23\times10^{-3}$ mm²/s) (Fig. 2). When we compared ADCs of lymphomas and bronchogenic carcinomas, there was no significant difference in the mean ADCs with an overlap between these two subgroups (p=0.36). A high ADC ($1.8\pm0.67\times10^{-3}$ mm²/s) was calculated in 1 patient with a lung cancer (adenocarcinoma) which would suggest the diagnosis of a benign mass.

The mean ADC for benign tumors was $2.04\pm0.67\times10^{-3}$ mm²/s (Fig. 3). The lowest ADC among benign tumors was detected in a patient with sarcoidosis ($1.41\pm0.59\times10^{-3}$ mm²/s). When we compared the ADCs from patients with sarcoidosis to those of other benign lesions, we found no significant difference (p=0.52), with the ADC readings from patients with sarcoidosis being lower. None of the measurements in patients with benign masses in general yielded a result below the cut-off value of $1.39\times$

10^{-3} mm²/s, which could lead to a misdiagnosis of malignancy.

ROC curve analysis

When using the cut-off value for ADC as $\leq 1.39\times10^{-3}$ mm²/s for the diagnosis of malignancy, the sensitivity and specificity were determined as 95% and 87%, respectively.

Discussion

Although DWI has been used to differentiate malignant and benign lesions in several other locations, DWI of the chest has been considered technically difficult for many years due to the physiologic motion artifacts caused by respiration and cardiac motion [10]. The adverse effects of motion can be reduced by using breath-hold and pulse triggered sequences. We thus obtained images using SS-SE-EPI sequences and breath holding. In addition, parallel imaging (SENSE) was utilized in our study to reduce distortion.

Our results suggest that the mean ADC of malignant mediastinal lesions is significantly lower than that of benign masses ($p<0.001$). Our search of the literature revealed the scarcity of such attempts in using DWI for this purpose. A report by Abdel Razek et al. [12] also showed a lower mean ADC for malignant compared to benign mediastinal masses with the threshold value of 1.56×10^{-3} mm²/s.

With regards to lung masses in general, there are still only a limited number of studies that have been conducted to evaluate the role of DWI [13–18]. Some of these studies chose not to evaluate ADCs probably because of susceptibility artifacts [14, 15, 17, 18]. Uto et al. [16] stated that lesion-to–spinal cord ratio was more effective ($p<0.001$) for differentiation between lung cancer and benign lesions. They found no significant difference between the mean ADCs ($p<0.388$). Mori et al. [14] found a significant difference between malignant and benign lesions using an ADC cut-off value of 1.1×10^{-3} mm²/s. Liu et al. [13] also observed the same trend with their reported mean ADC of 1.4×10^{-3} mm²/s as the threshold.

Two recent studies showed that metastatic mediastinal lymph nodes demonstrate a lower ADC than benign nodes [19, 20].

In our study, one patient with a mediastinal mass due to lung adenocarcinoma was misdiagnosed due to an ADC value higher than the cut-off value of 1.39×10^{-3} mm²/s. The lesion showed no apparent visual sign of necrosis. The discrepancy may result from the loose cellular arrangement of this particular tumor which may have enabled somewhat unrestricted diffusion.

The heterogeneity of the masses investigated with a wide spectrum of diseases and histopathological types is one of the limitations of this study. Further studies focused on specific types of tumors are recommended. Furthermore, susceptibility artifacts associated with echo-planar imaging sequences can be prohibitive for chest imaging. The variations in the main field caused by susceptibility can result in image nonuniformities including distortion. These artifacts especially occur near the air-tissue interfaces of the thoracic wall. In addition, susceptibility artifacts increase with the main magnetic field strength and are more prominent on 3 T systems compared with 1.5 T MRI. Our study with the parallel imaging technique used might have resulted in such artifacts being manifested to a lesser degree due to the shorter echo train lengths that could be employed.

We suggest that ADC measurements on DWI may help in differentiating malignant from benign mediastinal masses noninvasively.

References

1. Laurent F, Latrabe V, Lecesne R, Zennaro H, Airaud JY, Rauturier JF, Drouillard J (1998) Mediastinal masses: diagnostic approach. Eur Radiol 8:1148–1159
2. Strollo DC, Rosado-de-Christenson ML, Jett JR (1997) Primary mediastinal tumors: part 1: Tumors of the anterior mediastinum. Chest 112:511–522
3. Strollo DC, Rosado-de-Christenson ML, Jett JR (1997) Primary mediastinal tumors: part II. Tumors of the middle and posterior mediastinum. Chest 112:1344–1357
4. Whitten CR, Khan S, Munneke GJ, Grubnic S (2007) A diagnostic approach to mediastinal abnormalities. Radiographics 27:657–671
5. Tomiyama N, Honda O, Tsubamoto M, Inoue A, Sumikawa H, Kuriyama K, Kusumoto M, Johkoh T, Nakamura H (2009) Anterior mediastinal tumors: diagnostic accuracy of CT and MRI. Eur J Radiol 69:280–288
6. Ahn JM, Lee KS, Goo JM, Song KS, Kim SJ, Im JG (1996) Predicting the histology of anterior mediastinal masses: comparison of chest radiography and CT. J Thorac Imaging 11:265–271
7. Kawashima A, Fishman EK, Kuhlman JE, Nixon MS (1991) CT of posterior mediastinal masses. Radiographics 11:1045–1067
8. Puderbach M, Hintze C, Ley S, Eichinger M, Kauczor HU, Biederer JMR (2007) Imaging of the chest: a practical approach at 1.5 T. Eur J Radiol 64:345–355
9. Kauczor HU, Kreitner KF (2000) Contrast-enhanced MRI of the lung. Eur J Radiol 34:196–207
10. Tanaka R, Horikoshi H, Nakazato Y, Seki E, Minato K, Iijima M, Kojima M, Goya T (2009) Magnetic resonance imaging in peripheral lung adenocarcinoma correlation with histopathologic features. J Thorac Imaging 24:4–9
11. Ohno Y, Sugimura K, Hatabu H (2002) MR imaging of lung cancer. Eur J Radiol 44:172–181
12. Abdel Razek A, Elmorsy A, Elshafey M, Elhadedy T, Hamza O (2009) Assessment of mediastinal tumors with diffusion-weighted single-shot echo-planar MRI. J Magn Reson Imaging 30:535–540
13. Liu H, Liu Y, Yu T, Ye N (2010) Usefulness of diffusion-weighted MR imaging in the evaluation of pulmonary lesions. Eur J Radiol 20:807–815
14. Mori T, Nomori H, Ikeda K (2008) Diffusion-weighted magnetic resonance imaging for diagnosing malignant pulmonary nodules/

masses. Comparison with positron emission tomography. J Thorac Oncol 3:358–364
15. Matoba M, Tonami H, Kondou T, Yokota H, Higashi K, Toga H, Sakuma T (2007) Lung carcinoma: diffusion weighted MR imaging—Preliminary evaluation with apparent diffusion coefficient. Radiology 243:570–577
16. Uto T, Takehara Y, Nakamura Y, Naito T, Hashimoto D, Inui N, Suda T, Nakamura H, Chida K (2009) Higher sensitivity and specificity for diffusion weighted imaging of malignant lung lesions without apparent diffusion coefficient quantification. Radiology 252:247–254
17. Satoh S, Kitazume Y, Ohdama S, Kimula Y, Taura S, Endo Y (2008) Can malignant and benign pulmonary nodules be differentiated with diffusion-weighted MRI? AJR Am J Roentgenol 191:464–470
18. Qi LP, Zhang XP, Tang T, Li J, Sun YS, Zhu GY (2010) Using diffusion-weighted MR imaging for tumor detection in the collapsed lung: a preliminary study. Eur Radiol 19:333–341
19. Nakayama J, Miyasaka K, Omatsu T, Onodera Y, Terae S, Matsuna Y, Cho Y (2010) Metastases in mediastinal and hilar lymph nodes in patients with non-small cell lung cancer: quantitative assessment with diffusion weighted magnetic resonance imaging and apparent diffusion coefficient. J Comput Assist Tomogr 34:1–8
20. Kosucu P, Tekinbas C, Erol M, Sarı A, Kavgacı H, Öztuna F, Ersöz Ş (2009) Mediastinal lymphnodes:assessment with diffusion-weighted MR imaging. J Magn Reson Imaging 30:292–297